Journal of Environmental Chemical Engineering 11 (2023) 109451

Contents lists available at ScienceDirect

Journal of Environmental Chemical Engineering

journal homepage: www.elsevier.com/locate/jece

C-N co-doped titanium dioxide. Key aspects in the assessment of the air pollutants abatement capability

Alessia Zollo [a], Stefano Livraghi [a,*], Elio Giamello [a], Andrea Cioni [b], Valentina Dami [b], Giada Lorenzi [b], Giovanni Baldi [b]

[a] Dipartimento di Chimica and NIS, Università di Torino, Via P. Giuria 7, 10125 Torino, Italy
[b] COLOROBBIA CONSULTING S.r.L., Via Pietramarina 53, Sovigliana, 50053 Vinci, FI, Italy

ARTICLE INFO

Editor: Yunho Lee

Keywords:
Photocatalysis
Visible light
Indoor
TiO_2
C, N co-doping
NOx

ABSTRACT

In this work titanium dioxide modified by the simultaneous presence of both carbon and nitrogen dopants (C-N/TiO_2) has been prepared (starting from a commercial TiO_2 multiphasic matrix) and characterized according to two distinct lines of comparison, namely a) the typology of chemicals used in the doping and, b) the type of visible light (monochromatic or polychromatic) used to irradiate the solid. Singly doped systems C/TiO_2 and N/TiO_2 have also been prepared and compared to the co-doped one. All materials have been characterized by X-ray diffraction, UV–VIS spectroscopy and EPR (Electron Paramagnetic Resonance). The air pollutants remediation capability was evaluated by means of nitric oxide (NO) abatement tests according to the standard ISO 22197–1. Photoactivity of the pristine matrix is not modified by the presence of carbon (C/TiO_2) while it markedly increases when nitrogen is present (N/TiO_2 and C-N/TiO_2) confirming an essential role of this element in VLA photocatalytic systems. The photocatalytic tests indicate that the Illumination with monochromatic blue light is much more effective than that using a white LED light, which however represents a more common light source in indoor or occupational contexts. The effect of milling (a procedure often used to prepare photocatalytic devices for indoor air remediation) on the activity of the photocatalysts is slightly detrimental on the catalytic performances which however remain good enough to allow practical applications.

1. Introduction

Since the seminal paper of R. Asahi in 2001 [1] concerning the photocatalytic activity under visible light of N-doped TiO_2, the last two decades have seen an intense research activity devoted to the modification, or doping, of photoactive oxides with non-metals in order to obtain efficient Visible Light Active (VLA) photocatalysts. Nitrogen, carbon and fluorine are the most interesting elements investigated to dope metal oxides and in particular TiO_2 [2–7], and to date several commercial products are available, as in the case of the nitrogen doped TiO_2 (N-TiO_2) from Colorobbia (WO 2019/ 211787) [8].

The modification of photoactive oxides can involve either the bulk of the solid or its surface and, in some cases, both locations. Lattice modifications with an hetero-element can basically be of two types, substitutional, when the non-metal dopant takes the position of oxygen in the lattice, and interstitial when it is located in the empty spaces of the lattice. For instance, in the case of nitrogen-doped titanium dioxide, wet chemistry methods usually lead to interstitial forms of doping with nitrogen close and covalently bound to a lattice oxygen, while with high energy procedures such as the oxidation of nitrides or the nitridation of the oxide with ammonia, the substitutional form in the oxygen position is favoured [9]. Introducing carbon in the oxide lattice, an even wider range of possibilities is contemplated [10]. In any case, for both elements, the introduction of heteroatoms in the lattice of titanium dioxide (whose band gap energy is around 3 eV corresponding to ultraviolet frequencies) extends the light absorption to the visible range. This is due to the formation of energy states located between the valence band (VB) and the conduction band (CB) from which electron promotion into the CB is induced by photons with lower energy than the ultraviolet ones [8,11].

As far as surface modifications are concerned, the situation is less defined as it ranges from anchoring either carbonaceous species of various complexity or more ordered structures such as graphene or C_3N_4 [12,13]. For instance, in the case of the well-known VLA material

* Corresponding author.
E-mail address: stefano.livraghi@unito.it (S. Livraghi).

https://doi.org/10.1016/j.jece.2023.109451
Received 9 November 2022; Received in revised form 9 January 2023; Accepted 5 February 2023
Available online 7 February 2023

KRONOClean7000 the activation with visible light is attributed to the presence at the surface of carbon containing species with aromatic character and not to substitutional or interstitial carbon [14–16]. In general, these surface species act as antenna centres for the absorption of visible light or affect the lifetime of the photoinduced charge carriers.

In the present work we intend to show how a commercial TiO_2 system (PARNASOS® PH000025, COLOROBBIA CONSULTING S.r.l., Vinci, Italia) can be easily sensitised to the visible light via nitrogen and/or carbon doping and how practical aspects of both the material preparation (namely the chemical nature of dopants) and the conditions of the photocatalytic tests (monochromatic or polychromatic light) can affect the photoactivity results. For this purpose, three differently modified systems have been prepared using an equivalent amount of C/N containing dopant sources. Ammonium citrate has been selected as carrier of both N and C dopants, ammonia as carrier of nitrogen only, ethyl citrate as carrier of carbon. The last molecule has been selected since it is similar to ammonium citrate but with non-ionic character.

In the first part of the paper the characterization of the modified TiO_2 systems will be illustrated in order to find evidence of the species responsible of visible light activity. In the second part, the photocatalytic activity under visible irradiation of the modified systems is compared using the reaction of nitric oxide (NO) abatement, a benchmark test adopted by EU regulations to compare photocatalysts working in gaseous atmosphere.

Concerning the photocatalytic activity under visible light, two main experimental parameters have been considered. The first one is, as already mentioned, the type of light employed in the tests. For the practical application of VLA photocatalysts in indoor contexts, in fact, the use of visible light irradiation is highly recommended. However, at laboratory level, the choice of the irradiation source is usually made on the basis of the optical absorption properties of the VLA material (monochromatic sources, filtered UV–Vis lamp and so on). This choice does not always reproduce the illumination usually adopted in indoor or occupational environment. For this reason, two different light sources have been tested in this work, a blue Light Emitting Diode (LED), whose wavelength corresponds to the maximum absorption in the visible range of the systems prepared in this work, and a white LED, more common in indoor or occupational contexts.

A second parameter concerns the ball milling procedure, which is commonly adopted in the preparation of photoactive phases [17, 18, 19, –20], but also as a post synthesis process. The latter procedure (poorly investigated in the literature) has the dual purpose of increasing the surface area and of obtaining a stable suspensions of the photocatalytic powders which is a crucial step for the functionalization of inert supports with the photocatalyst in commercial devices [21]. In the present work, the above described materials were submitted to ball milling in order to evaluate, by comparison with the non-milled solids, the effect of this treatment on their ultimate photocatalytic activity [22–24].

2. Materials and methods

2.1. Modified TiO_2

The doped and co-doped systems were obtained starting from a commercial TiO_2 suspension (PARNASOS® PH000025, COLOROBBIA CONSULTING S.r.l., Vinci, Italia) modified in three distinct ways with nitrogen and/or carbon using as dopant source NH_3, dibasic ammonium citrate ($C_6H_8O_7{\cdot}2NH_3$), and triethyl citrate ($C_{12}H_{20}O_7$) respectively. For each preparation an appropriate amount of dopant in order to get the same nominal N/Ti and C/Ti molar ratio has been employed (C/Ti = 0.11 and N/Ti = 0.035). In a typical synthesis the dopant was mixed with the starting commercial suspension and the resulting mixture was then recovered via spray-dry procedure. The final solid was then calcined at 743 K for 60 min using a heating rate of 6.2 K/min. The samples are identified according to the labels reported in Table 1.

2.2. Bare TiO_2

Bare TiO_2 was obtained recovering the solid from the same commercial TiO_2 suspension and submitting it to a calcination in air at 743 K for one hour (heating rate 6.2 K/min) in order to reproduce the thermal treatment employed to obtain the C/N modified samples (Section 2.1).

2.3. Ball milling procedure

A high-energy grinding system (High energy ball mill E-MAX, Retsch GmbH) was employed. The powders were dispersed in ethanol in order to obtain suspensions with titania concentration around 15% w/w, using yttria stabilized zirconia beads with 0.1 mm diameter as grinding medium. Ethanol has been selected since it is the liquid used in the large scale procedure of preparation of commercial photocatalyst from the same matrix [8] The milling time was 90 min and the speed used was 1500 min^{-1}. The samples are identified according to the label reported in Table 1.

2.4. X-Ray Diffraction (XRD)

Powder X-ray diffraction (XRD) patterns were recorded with a PANalytical PW3040/60 X'Pert PRO MPD diffractometer using a copper Kα radiation source. The diffraction patterns were obtained in the 2θ range between 20° and 80° and the X'Pert High-Score software was used for data handling. Diffraction patterns were refined with Rietveld method using MAUD (Material Analysis Using Diffraction) program [25].

2.5. Diffuse Reflectance spectroscopy (DRS)

The UV-Visible Diffuse Reflectance (DR-UV-Vis) spectra of the prepared solids were recorded using a Varian Cary 5000 spectrometer. A Polytetrafluoroethylene (PTFE) sample was used as the reference. The

Table 1
Phase composition and features of the materials prepared in the present work.

Sample description	Sample labelling	Anatase (%)	Rutile (%)	Brookite (%)	Anatase Crystallite (nm)	Rutile Crystallite (nm)	Brookite Crystallite (nm)	BG (eV)
Samples before milling								
Bare TiO_2	T	44	25	31	21	33	15	3.0
C-modified	TC	49	23	28	17	41	12	3.0
N modified	TN	41	24	35	18	32	15	3.0
C/N modified	TCN	28	52	20	21	48	9.3	2.9
Ball milled samples								
Bare TiO_2	Tm	26	20	54	23	13	7.1	3.0
C modified	TCm	28	22	50	18	12	5.8	3.0
N modified	TNm	25	19	56	22	12	6.7	3.0
C/N modified	TCNm	15	41	44	36	13	5.3	2.9

spectra were recorded in the 200–800 nm range at a scan rate of 240 nm/min with a step size of 1 nm. The measured reflectance was converted with the Kubelka-Munk function.

2.6. Attenuated total reflection infrared spectroscopy (ATR-IR)

Spectra were acquired on Perkin-Elmer Spectrum Two FT-IR spectrometer with the ATR accessory with a diamond cell and a MIR source (8000–30 cm^{-1}). ATR were obtained recording 16 scans between 800 and 4000 cm^{-1} at a resolution of 4 cm^{-1}.

2.7. Continuous Wave Electron Paramagnetic Resonance (EPR)

EPR spectra were acquired using a Bruker EMX spectrometer operating at X-band (9.5 GHz), equipped with a cylindrical cavity operating at 100 kHz field modulation. All the spectra were recorded at room temperature (RT) with a 1 mW of incident microwave power and with a modulation amplitude of 0.2 mT.

2.8. Photocatalytical NO abatement test

The NO abatement experiments were carried out in a photoreactor developed by Cericol (Fig. 1) [26] and designed according to the ISO 22197–1 standard [27]. This standard serves as a sound basis for measurements and its recommendations were largely followed for the practical conduction of the present study.

The system consists of a glass reaction chamber equipped with a quartz window, in which the environmental conditions are simulated in terms of concentration of contaminants, temperature and relative humidity. The device works in automatic and a dedicated software controls the flow of pollutant gas and the moisture. The photocatalytic efficacy was tested studying nitric oxides (nitrogen monoxide and/or nitrogen dioxide) degradation using a device measuring chemiluminescence (model 42i, Thermo).

The photoreactor allows performing the analysis either in continuous or discontinuous mode.

The first mode permits to perform the analysis in single step from the reaction chamber directly to the chemiluminescence. In this case, the inlet pollutant concentration remains constant during the entire analysis. The initial concentration of the chemical species is determined before switching-on the light. After turning on the light, a decrease is measured, whose value is proportional to the efficiency of the photocatalyst.

In the second mode, the reaction chamber is connected to a bag and to a peristaltic pump, in order to create a closed circuit. The bag works as reservoir from which it is possible to send the pollutant atmosphere to the measuring instrument. Regulating the sampling and the recirculation times, it is possible to obtain data to determine the kinetic of the degradation reaction.

Capability in NO abatement has been tested under two different irradiation conditions, i) upon blue light illumination obtained using a blue LED source with an incident irradiance of 58 W/m^2 (detection range 400–800 nm), ii) upon white light illumination obtained using a white (3000 K) LED source with an incident irradiance of 87 W/m^2 (detection range 400–800 nm). In a typical test, each powder obtained from the calcination process was used to prepare a 5% w/w water suspension, which was applied on a glass piece via spray-gun, with an active sample area of 100 mm ± 0.10 mm in width and 100 ± 0.10 mm in length. Approximately 0.15 g of dry product was employed in each test.

Each suspension obtained from the milling process was deposited by spray-gun on a glass sheet, with an active sample area of 100 mm ± 0.10 mm in width and 100 ± 0.10 mm in length.

The analyses were performed using the discontinuous mode, consisting in six samplings of 5 min each, alternated with 15 min of recirculation, for a total time of analysis of 105 min.

The dry air, moist air and nitric oxide were mixed in proportions such as to obtain a fixed nitric oxide concentration of around 500 ± 50 ppbv in an atmosphere having about 50 ± 10% of relative humidity at a temperature of about 25 ± 5 °C.

3. Results

3.1. Structural and optical characterization

Table 1 summarizes the main structural features of the samples studied in this work. Fig. 2 (panel A) shows the XRD powder patterns of the samples before milling. The corresponding phase composition is reported in Table 1. Interestingly, as it will be discussed later, pristine TiO_2 is composed by three different crystallographic phases, anatase, rutile and brookite. The modification of this solid does not introduce relevant differences from the point of view of the phase composition except for the case of the TCN system for which the conversion of a fraction of both anatase and brookite into the thermodynamically favoured rutile phase [28] is observed.

Fig. 1. Landscape picture of the photoreactor.

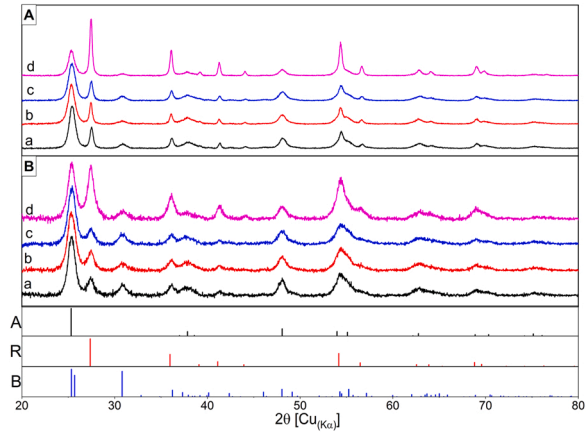

Fig. 2. XRD pattern. Panel A: samples before milling. a = T, b = TC, c = TN, d = TCN. Panel B: ball milled samples. a = Tm, b = TCm, c = TNm, d = TCNm. In the lower part the expected patterns for the TiO_2 polymorphs, A= anatase (ICSD: 01–086–1157), R = rutile (ICSD: 01–086–0148) and B = brookite (ICSD: 01–076–1937). The corresponding composition are reported in Table 1.

The optical properties of the samples before milling are reported in Fig. 3 (panel A). All spectra are dominated by the typical absorption in the UV region due to the electronic transition between the valence band and the conduction band of TiO_2. The Band Gap values (E_g) evaluated via the Tauc's plot method are about 3.0 eV for all samples (see Table 1). This value is the same reported for the rutile polymorph suggesting that the optical absorption mainly depends on this polymorph. The bare titanium dioxide matrix (sample T) is also characterized by a weak absorption tail which reaches the visible light range. Such an absorption is still due to the rutile component as in the case of other systems containing this phase, for instance the well-known P25-Envonik (see the Supporting Information, hereafter S.I.) [29]. The insertion during the synthesis of the carbon and nitrogen dopants modifies the absorption in the visible region. The TC sample shows again a weak absorption tail however extended, in this case, to the whole visible region while the TN sample shows a more defined absorption shoulder in the range 400 – 500 nm (Fig. 3A curve b and c). The more relevant effect is observed in the case of the TCN material for which the optical absorption in the visible is by far higher than that of the other doped samples. This can be due to the presence, in this case, of two added elements (C and N) but also to a superior capability of the compound used to modify the system (ammonium citrate) to interact with the TiO_2 matrix, thus affecting the total amount of carbonaceous species loaded at the surface. Two different citrates (the ammonium salt and the ester) in fact, lead to a dramatic difference in terms of visible light absorption, much higher in the case of the ammonium citrate (Fig. 3. Panel A). This different behaviour is tentatively ascribed to a stronger interaction of the ammonium salt with the oxide surface due to its ionic character, with respect to the organic ester for which a weaker interaction with the solid matrix is likely involved, affecting thus the decomposition pathway during the calcination. In order to confirm the key role of the ionic character of the precursor in determining the amount of carbon containing residual species a further, "ad hoc" preparation has been performed using sodium citrate (See S.I.). Using sodium citrate, the optical properties are similar to those of the TCN system.

Upon ball milling, a change in the ratio of the TiO_2 polymorphs occurs in parallel with a decrease of the crystallites size. The amount of rutile phase remains almost unchanged whereas that of the brookite polymorph increases at the expense of the anatase one. This is due to the high energy involved in the ball milling procedure that causes a partial conversion of anatase which however is not sufficient to convert this phase into the most thermodynamically stable rutile one. In other words, brookite represents an intermediate phase in the mechanically induced anatase-to-rutile phase transformation as also reported in the literature [30,31]. The ball milling procedure also affects the optical properties of the starting materials in the visible region (Fig. 3B), while the intrinsic band gap transition does not change. In detail, sample T shows a new absorption feature, clearly visible in the region 400 – 550 nm whereas for the TC and TN materials no significant modification can be observed. In the case of sample TCN, the milling process induces a drastic decrease of the initial absorption in the visible region which, however, remains higher than those of the other doped materials. This last experimental evidence clearly indicates that in the case of TCN, ball milling partially removes the species responsible for the visible light absorption. It can be thus inferred that the removed species have surface nature.

The effects of the milling procedure are not limited to the partial removal of surface compounds observed in the case of TCN. Some new organic moieties are in fact left at the surface of the materials after milling as revealed by Infra-red analysis (Fig. 4). The figure in fact points out that the samples before milling show two spectroscopic features only, the broadened absorption around 3000 cm^{-1} due to surface hydroxyl groups and adsorbed water and a second features centred at 1635 cm^{-1} due to the molecular water deformation mode [32]. Features related to the presence of the dopant are undetectable in the three cases. After milling in liquid phase (ethanol) the IR pattern becomes more complex. The previously described features due to OH and H_2O increase, and a triplet appears in the region (2850 – 2990 cm^{-1}) due to aliphatic C-H [33]. A complex vibrational pattern appears also in the region between 1500 cm^{-1} and 1000 cm^{-1}. In this region carbonate-like species and aliphatic C-H bending modes are expected [34]. Summarising, the ball milling procedure not only affects the particle size of the materials but also modifies the optical properties and the chemical surface composition of the samples, the latter modification being due to the effect of the organic medium used in the milling procedure.

3.2. EPR characterization

The CW-EPR technique can be adopted to characterize nature and features of the photoactive center in C/N modified TiO_2. With this technique, it is possible in fact to monitor the solids either in the dark or under irradiation unravelling, in this second case, the features of excited states. It was shown, for instance, that in the case of titanium dioxide doped with nitrogen, paramagnetic centers form in the bulk of both anatase and rutile and that one of these species (interstitial N, formally NO^{2-}) plays a decisive role in the photochemistry of the system under visible light [7]. This species, whose concentration is affected by irradiation with visible light, is in fact responsible of photoinduced electron transfer at the surface and can be therefore individuated as a photoactive species. The species is characterized by a rhombic **g** tensor whose components span over the range 2.007–2.003, and by a hyperfine triplet

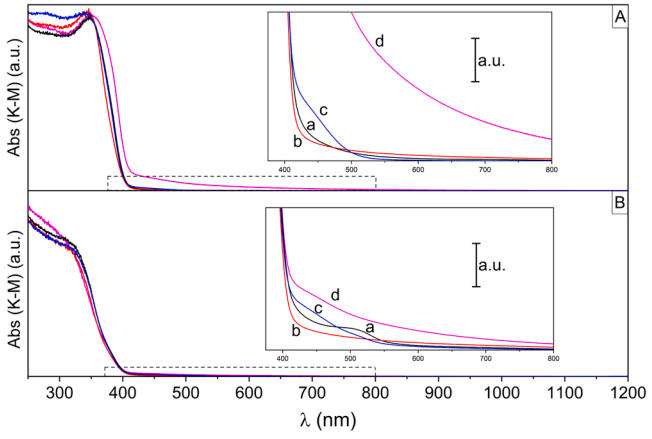

Fig. 3. DRS spectra. Panel A: samples before milling. Panel B: ball milled samples. Line a = T, b = TC, c =TN, d = TCN. The corresponding Band Gap (GB) evaluated via the Tauc's plot are reported in Table 1.

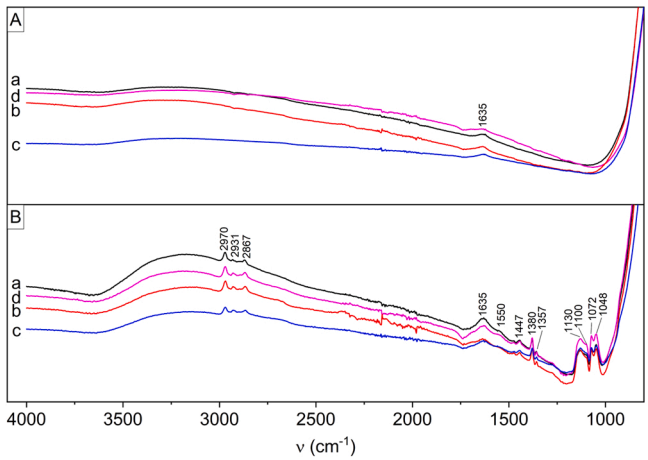

Fig. 4. ATR spectra. a = T, b = TC, c = TN, d = TCN. Panel A. Samples before milling. Panel B: ball milled samples.

due to the interaction of the unpaired electron with the nucleus of ^{14}N isotope (nuclear spin I = 3/2, expected lines 2I+1 =3). The **g** tensor of the N species is poorly informative being the three principal values close one to each other while the hyperfine interaction shows a main coupling in one direction (A = 3.27 mT in Fig. 5) that can be considered the fingerprint of such a species.

Similarly, for a TiO_2 material doped with carbon, E.A. Konstantinova et al. reported the presence of a carbon-based paramagnetic center whose spectral intensity depends on the irradiation conditions [35]. In that case, the signal is characterized by an isotropic line shape with a g factor close to that of the free electron (g_e = 2.0023) and no hyperfine coupling are observed since the most abundant isotope (^{12}C) has I = 0. The EPR spectra recorded in the dark of the materials synthetized for this work are shown in Fig. 4. The bare material (T) does not show, as expected, any paramagnetic signal while, after the modification, the EPR signals above introduced show up. Sample TC shows an isotropic signal centered at g= 2.002 due to C containing species while the TN material shows a more intense signal amenable to the previously discussed interstitial nitrogen in TiO_2 (NO^{2-}) [36,37]. The TCN sample shows a more complex EPR spectrum based on the overlap of the two already described signals indicating the simultaneous presence of both the previously discussed species (C-based and N-based respectively). The former has a prominent role in quantitative terms, as also indicated by the optical absorption which is qualitatively similar for the two samples TC and TCN but more intense in the case of the co-doped system. The ionic dopant (ammonium citrate) is therefore more efficient in forming photosensitive phases though apparently less efficient than NH_3 in introducing N into the TiO_2 lattice. (Figs. 3 and 5).

3.3. NO abatement test

Nitrogen oxides are a family of poisonous, highly reactive gases. These gases form when fuel is burned at high temperatures. NOx pollution is emitted by automobiles, trucks and various non-road vehicles (e.g., construction equipment, boats, etc.) as well as industrial sources such as power plants, industrial boilers, cement kilns, and turbines. Nitrogen oxides have a significant impact on the ozone layer and are significant greenhouse gases and cause acid rain. The impacts of NOx on human health include damage to the lung tissue, breathing and respiratory problems.

To date, a number of researchers have investigated the dynamics of the photocatalysis of nitrogen oxides. Photocatalytic oxidation (PCO) based on the use of titanium dioxide is an attractive proposition due to its ease of use, instant impact and low cost when compared with other methods for ambient NOx removal [38].

The capability to remove contaminants such as NO in the presence of a gaseous phase simulating the atmosphere composition (O_2, N_2 and H_2O) was investigated using two different light sources (see experimental section). In a typical test, beside the abatement on the NO molecule, the formation of the NO_2 intermediate is also followed since Nitrogen(II) and Nitrogen(IV) oxides, considered together as NOx, are very harmful for the life organisms and for this reason both these species must be monitored during the test for the correct assessment of the pollutant abatement.

In order to evaluate the data reported in this Section, it has to be taken in mind a possible contribution to NO conversion of the two following non photoinduced reactions (i.e. occurring also in dark conditions).

$$2NO + O_2 \rightarrow 2NO_2 \quad (1)$$

$$2NO_2 + H_2O \rightarrow HNO_2 + HNO_3 \quad (2)$$

The presence of such processes on the TiO_2 surface in fact has been reported in the literature in some studies devoted to monitoring NO absorption in dark conditions [39,40].

The following figures report the results of NO abatement under irradiation with white LED (Figs. 6 and 7) and blue LED (Figs. 8 and 9) of the samples before milling (Figs. 6 and 8) and after milling (Figs. 7 and 9) respectively. A first scrutiny of the figures indicates a non-negligible photoactivity of the undoped matrices (T and Tm) which can be ascribed to the above mentioned dark reactions (1,2) and, tentatively, to a second factor, namely an intrinsic visible light photocatalytic activity of the pristine titania here employed which is a complex triphasic system (Table 1) reminiscent of the well-known and extremely active Evonik P25 material. This effect, which in any case remains a partial contribution to the whole reactivity of the doped systems, will not be discussed further since it is out of the purposes of the present paper. By the way, and analogously to Evonik P25 (see S.I.), the optical absorption of T and Tm indeed shows a shoulder in the visible region (Fig. 2).

Under illumination, a series of further reactive steps triggered by the photoinduced charge carriers are expected, namely [41,42]: i) charge carrier separation and formation of reactive oxygen species (reactions 3

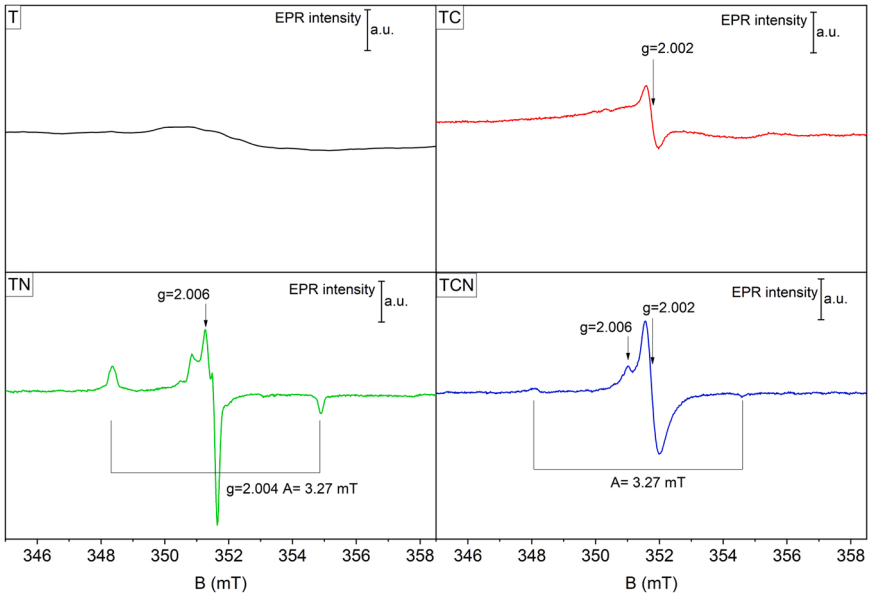

Fig. 5. CW-EPR spectra of the samples before milling.

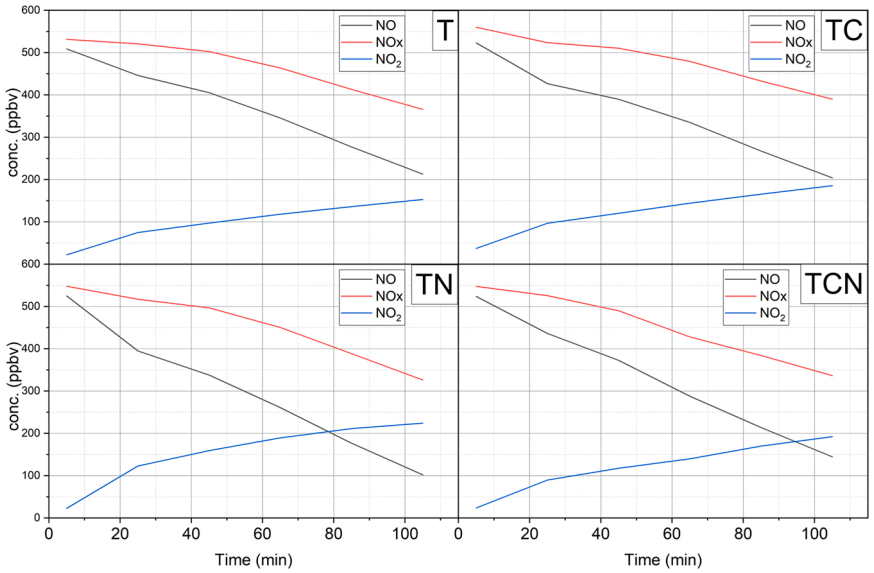

Fig. 6. NO abatment on the samples before milling upon white LED illumination.

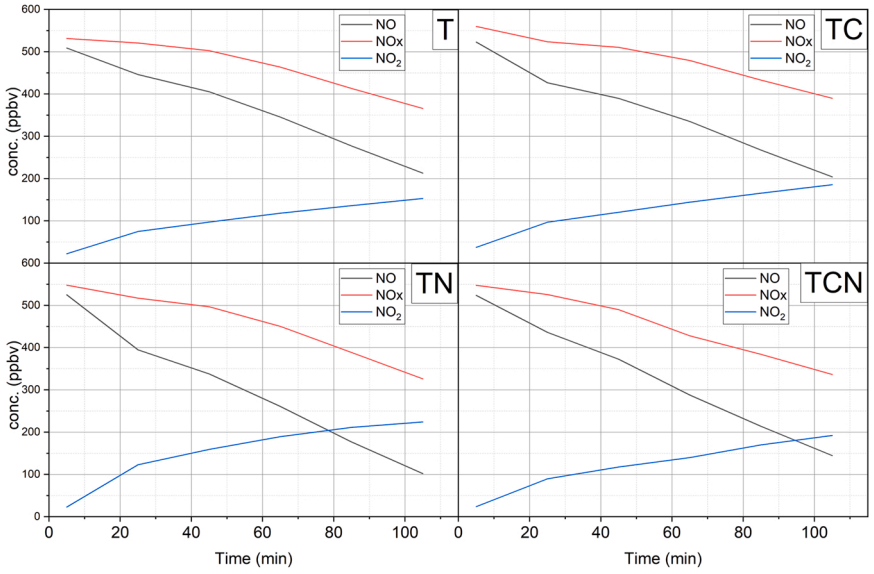

Fig. 7. NO abatment on the milled samples upon white LED illumination.

– 5), ii) partial oxidation of NO leading to NO_2 or HNO_2 (reactions 6 and 7), iii) full oxidation to NO_3^- or HNO_3 (reactions 8 – 9).

$$TiO_2 + h\nu \rightarrow TiO_2\ (h^+; e^-) \quad (3)$$

$$H_2O + h^+ \rightarrow {}^\bullet OH + H^+ \quad (4)$$

$$O_2 + e^- \rightarrow O_2^{\bullet -} \quad (5)$$

$$NO + 2{}^\bullet OH \rightarrow NO_2 + H_2O \quad (6)$$

$$NO + NO_2 + H_2O \rightarrow 2HNO_2 \quad (7)$$

$$NO_2 + {}^\bullet OH \rightarrow HNO_3 \quad (8)$$

$$NO + O_2^{\bullet -} \rightarrow NO_3^- \quad (9)$$

In the following section the NO degradation capability of the pristine and modified systems using either white or blue light is reported.

3.3.1. NO abatement under white LED illumination

Figs. 6 and 7 refer to the samples before milling (Fig. 6) and the milled ones (Fig. 7) under white LED illumination. The emission spectrum of the light source covers a wide range in the visible wavelengths region, between 400 nm and 800 nm (see S.I.), and in principle is able to exploit the whole absorption features of the samples, and, not less important, represents a typical illumination in indoor contexts. The abatement of NO (black line) involves two processes, namely its oxidation to gaseous NO_2 (blue line) and the oxidation to non-gaseous compounds (nitrites and nitrates) thus removed from the atmosphere. For this reason, it is convenient to evaluate the actual activity of each system considering this second fraction that is reported in the Figures in terms of overall NOx abatement (red lines). Considering in particular the whole abatement of gaseous oxides (NOx, red lines), the following trend of activity can be identified for the samples before milling T ≈ TC<TN≈TCN, while the generation of the oxidation intermediate (NO_2) remains almost the same in all cases (Fig. 6 and Table 2). In detail, the modification with carbon (sample TC) does not seem to introduce

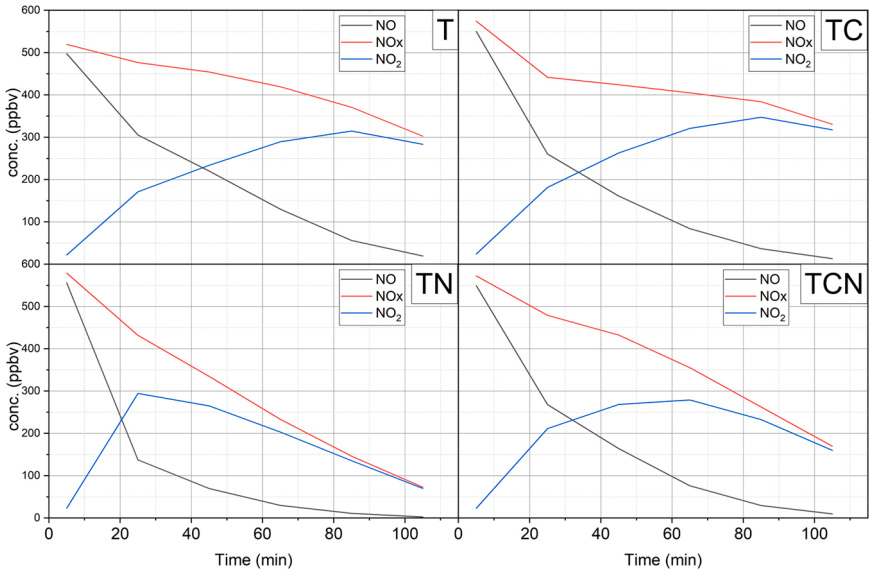

Fig. 8. NO abatment on the samples before milling upon blue LED illumination.

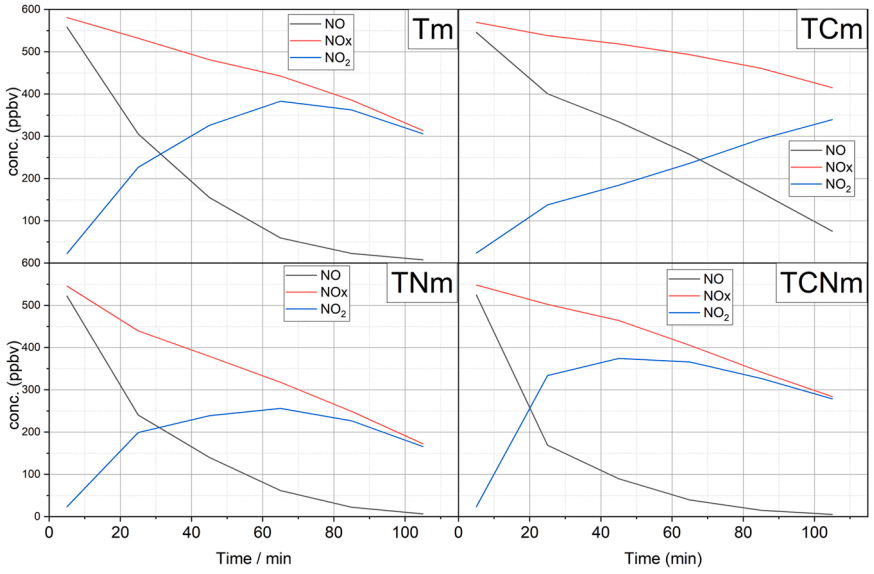

Fig. 9. NO abatement on the milled samples upon blue LED illumination.

Table 2
NO gas decomposition activity of samples after 105 min, under the two different light sources employed in this work.

	T	Tm	Tc	TCm	TN	TNm	TCN	TCNm
White LED								
% NOx degr.	31	41	31	30	41	34	39	29
% (NO →NO_2)	44	45	47	37	48	43	44	68
Blue LED								
% NOx degr.	42	46	42	27	87	68	70	48
% (NO→NO_2)	57	55	58	62	13	32	29	53

significant improvements in the photooxidation of NO. In this case, in fact, the total abatement of the pollutants (NOx) and the amount of photogenerated NO_2 are almost the same of the corresponding pristine sample T. For both nitrogen containing samples (TN, TCN), a slightly higher abatement of NOx is observed suggesting a role of nitrogen doping in improving the photocatalytic activity. In these two samples, the photodegradative pathway (reaction 8 – 9) more significantly contributes to the overall activity which, however, is only weakly improved by the doping process. As far as the milled samples are concerned, a worsening of the photoactivity for the samples TN and TCN is observed (Fig. 7). This experimental evidence can be attributed to a further and detrimental carbon contamination occurring during the milling process as evidenced by the IR bands (Fig. 4). In the case of the bare sample Tm only, the total NOx abatement is slightly higher as the milling contamination is less effective on the undoped material (T). In the case of TCNm the NO concentration actually drops close to zero but this positive effect is cancelled by the NO_2 concentration that reaches its maximum value (Fig. 7) so that the total NOx abatement is not improved. Data here reported indicate that, even though both modifications with carbon and nitrogen introduce energy states in the materials extending the optical properties to the visible light range, the most relevant role seems to be associated to the presence of nitrogen. The higher activity is observed in fact for the samples TN and TCN.

3.3.2. NO abatement under blue LED illumination

By employing a monochromatic blue LED, in spite of the lower irradiance of the source (see S.I.), the photoactivity results are much more interesting with respect to those obtained using white light. For all samples (Fig. 8), differently from the case of white illumination (Fig. 6), only few traces of the initial NO are detected after 105 min of irradiation (Table 2). However, the formation of NO_2 is still relevant in the two cases of T and TC whose global performances (NO_x) are therefore similar to those observed under white illumination. Moreover, since the activities of T and TC are again very close to each other, the effect of doping with the only carbon source seems again ineffective despite the clear onset of a visible light absorption in the case of TC (Fig. 3). The same consideration can be drawn analysing the photoactivity of the sample prepared using sodium citrate as a dopant precursor (see S.I.). This material shows a relevant absorption in the visible region as in the case of the TCN sample, but its NO abatement capability does not differ significantly from that of TC or T samples. In this system therefore most of the species that contribute to the overall absorption in the visible light range, do not really contribute to the photoactivity in the same conditions. The photocatalytic activity of the two nitrogen containing samples (lower panels in Fig. 8 and Table 2) is definitely higher. The total NOx curves clearly indicate that in these two cases a more efficient total oxidation of the initial NO occurs, in particular for the sample modified using NH_3, as the NO concentration is close to zero after about 100 min and the NO_2 one attains the minimum value in this set of experiments. This confirms what previously inferred about the essential role of nitrogen in these systems. In one case N is introduced directly using an ammonia solution (TN) thus obtaining the most active material. The activity in NO abatement however is only slightly lowered if a co-doped material is prepared using an organic ammonium salt indicating that both modifications can be confidently adopted according to the convenience. As already observed and discussed in the case of white LED irradiation, also in this case, after milling, a general worsening of the photoactivity is observed (Fig. 9) still maintaining the trend in photoactivity observed for the samples before milling (T ≈ TC<TCN<TN) [7].

4. Discussion

The data here reported show how an extension of the photocatalytic activity to the range of the visible light can be easily achieved by simple chemical treatments modifying a commercially available TiO_2 powder. For the sake of clarity, it has to be recognized that the observed activity encompasses a partial contribution of the intrinsic, non negligible, activity of the polyphasic TiO_2 matrix (see before) and of that of the dark reactions (1) and (2). Nonetheless, the contribution of the dopants remains important (Table 2). We have also shown that the treatments necessary to insert the photocatalytic materials in a commercial device, i.e. ball milling in an organic liquid medium, reduce the performance of the solid at an extent that does not impede their practical application.

In all cases here studied, species active in the visible range are formed as indicated by both optical absorption and EPR. Absorption in the visible region is due to the presence of energy states from which electronic excitation can be originated by the action of visible light, and that are distributed differently in the various materials (Scheme 1). In the case of nitrogen doped TiO_2 the new energy levels are well known and mainly localized close to the valence band giving rise to a relatively sharp transition in the 400 − 500 nm range [7,9]. In the case of carbon, the modification of the electronic structure is less clear and certainly more complex since, in principle, both C-doping centres within the matrix and active interfaces between TiO_2 and surface carbonaceous species can be present. Whatever the structural organisation, a complex distribution of energy levels leads to the extension of the optical absorption over a wider range of wavenumbers (400–800 nm). The TCN sample shows the higher absorption ability of the whole set of samples. The optical absorption covers the entire visible range (400–800 nm) and it is qualitatively similar to that of the TC sample. The contribution of

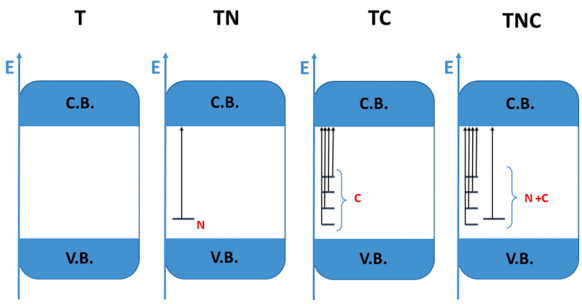

Scheme 1. Sketch of the electronic structure of the C/N modified photocatalysts compared with that of the pristine TiO_2. The contribution of carbon is schematically illustrated in terms of energy states between valence and conduction band only, neglecting if the states are due to bulk or surface C-containing species.

nitrogen doping (N is present in the system as firmly indicated by EPR results) is buried by the overwhelming absorption due to carbon species. Nonetheless the role of nitrogen is fundamental in the photocatalytic activity of the materials in the reactions of NO abatement.

The best photocatalytic activity (Table 2) is observed in fact for nitrogen containing materials (TN and TCN) pointing to a prominent role of the intra-band gap N states (NO^{2-}, monitored by EPR) in the generation of the charge carriers entailing the photocatalytic process. This is further evidenced when a system prepared using sodium citrate is analysed. For this material, in spite of a relevant absorption in the visible region, no significant difference in the activity with respect to the pristine T sample is observed (See S.I.). The higher photocatalytic activity obtained using monochromatic blue light confirms this point of view since the energy of the blue photons (around 2.7 eV) corresponds to the energy needed for the excitation of the NO^{2-} intra-band gap centers [9]. An effective synergy between C and N dopants has not been observed at least for the reaction here investigated (Figs. 8 and 9) though it cannot be excluded in the case of other reactions in gas phase on which our laboratories are still actively working. The somehow surprising result of a lower efficiency of the illumination with a polychromatic light source (Figs. 6 and 7) can be tentatively explained, as before mentioned, in terms of the efficiency of the selective excitation of NO^{2-}centers. The presence of a wide set of intra bad gap levels (see Scheme 1) together with that of a multiplicity of photon energies could easily entail a series of interactions detrimental for the whole photocatalytic activity.

Finally, as mentioned at the beginning of this Section, the activity of the materials is negatively affected by the post-treatment ball milling procedure that is required in case of some practical application of the materials [23]. Although the materials, as evidenced by diffractometric analysis, have nanometric size, after the calcination process, they appear as a 'soft' aggregate. The most suitable technique for breaking down this type of aggregates to obtain stable suspension is the ball milling. During this process the powder is subjected to high-energy collisions from the balls for getting well-dispersed slurries or suspensions. Such a process involves the dispersion of the particles in a liquid medium to neutralize the surface charges, and either water or alcohol can be used as dispersion medium, depending on the sample material.

Such a detrimental effect has already been observed in TiO_2 systems, and a general consensus ascribes the phenomenon to the generation of new phases, mainly amorphous TiO_2 and brookite, containing high amounts of defects [24–26]. The defects can act as recombination centres and the loss in photoefficiency offsets any gain due to the increase in surface area. It is also worth to mention that such studies were carried out grinding the powders without liquid medium or using water, and the photoefficiency was evaluated under UV light, making difficult a straightforward comparison. In the present case however a further parameter has to be considered that is the surface contamination due to

the alcohol employed as dispersion medium during ball milling procedure. Previous studies have shown in fact that photocatalytic activities in visible wavelength strongly depend on the solvent used: if the organic solvent causes surface contamination a worsening of the photoactivity is expected [43]. The presence of organic moieties is in fact clearly evident by the ATR analysis (Fig. 4). These residues cannot improve the visible light absorption due to their aliphatic nature but can hamper the interaction of substrates with the oxide surface. This effect could be attenuated by treatments on the ground materials aimed at removing the excess of organic matter deposited at the surface during milling. This point also is currently under investigation in our laboratories.

5. Conclusion

Summarizing, we have prepared three photoactive systems doping a multiphasic TiO_2 matrix with different dopants namely using an organic ester (ethyl citrate, C doping), a corresponding organic ammonium salt (ammonium citrate, C-N doping) and ammonia (N doping). Even though carbon modification is reported to be an efficient way to improve the TiO_2 photoactivity, for the systems analysed in this work the presence of nitrogen plays a crucial role in dictating the final properties of the photocatalysts. A significant difference in photoactivity is observed comparing the results obtained using a blue light, whose wavelength corresponds to the maximum absorption in the visible range of the systems prepared in this work, and a white LED, more common in indoor or occupational contexts. These results clearly indicate that the choice of the correct light source is crucial to understand the activity in indoor applications, this because the common illumination in occupational contexts may not coincide with the best absorption properties of the material. Finally, the effect of ball milling procedure has also been evaluated. A slight worsening of the photoactivity, in terms of NOx decreasing, is observed caused by the grinding procedure that does not preclude the applications of the materials in devices for pollutant abatement. In some cases, as the TCN sample of the present work, the fading of the photocatalytic activity could also be amenable to a second factor, i.e. the removal by mechanical action of superficial active species.

CRediT authorship contribution statement

Alessia Zollo: Investigation, materials characterization and data elaboration. **Stefano Livraghi:** Conceptualization, development of the methodology and writing the original draft. **Elio Giamello:** Conceptualization, writing the original draft. **Andrea Cioni:** Investigation, material preparation. **Valentina Dami:** Investigation, performing the NO test. **Giada Lorenzi:** Investigation, performing the NO test. **Giovanni Baldi:** Project administration.

Declaration of Competing Interest

The authors declare that they have no known competing financial interests or personal relationships that could have appeared to influence the work reported in this paper.

Data Availability

Data will be made available on request.

Acknowledgments

This paper is a part of the project that has received funding from the Compagnia di San Paolo, Torino with the project SusNANOCatch “sustainable strategies to reduce the presence in the environment of nanoparticle deriving from depollution process”. The Authors thank the Italian MIUR through the PRIN Project 20179337R7, Multi-e “Multi electron transfer for the conversion of small molecules: an enabling technology for the chemical use of renewable energy”.

Appendix A. Supporting information

Supplementary data associated with this article can be found in the online version at doi:10.1016/j.jece.2023.109451.

References

[1] R. Asahi, T. Morikawa, T. Ohwaki, K. Aoki, Y. Taga, Visible light photocatalysis in nitrogen doped titanium oxide, Science 293 (2001) 269–271.
[2] H. Yu, M. Zhang, Y. Wang, J. Lv, Y. Liu, G. He, Z. Sun, Low-temperature strategy for vapor phase hydrothermal synthesis of C\N\S-doped TiO_2 nanorod arrays with enhanced photoelectrochemical and photocatalytic activity, J. Ind. Eng. Chem. 98 (2021) 130–139.
[3] N.R. Khalida, A. Majida, M. Bilal Tahira, N.A. Niazb, Sadia Khalid, Carbonaceous-TiO_2 nanomaterials for photocatalytic degradation of pollutants: A review, Ceram. Int. 43 (2017) 14552–14571.
[4] P.S. Basavarajappa, S.B. Patil, N. Ganganagappa, K.R. Reddy, A.V. Raghu, Ch. V. Reddy, Recent progress in metal-doped TiO_2, non-metal doped/codoped TiO_2 and TiO_2 nanostructured hybrids for enhanced photocatalysis, Int. J. Hydrog. Energy 45 (2020) 7764–7778.
[5] M.V. Dozzi, C. D'Andrea, B. Ohtani, G. Valentini, E. Selli, Fluorine-doped TiO_2 materials: photocatalytic activity vs time-resolved photoluminescence, J. Phys. Chem. C. 117 (2013) 25586–25595.
[6] V. Trevisan, A. Olivo, F. Pinna, M. Signoretto, F. Vindigni, G. Cerrato, C.L. Bianchi, C-N/TiO2 photocatalysts: effect of co-doping on the catalytic performance under visible light, Appl. Catal. B: Environ. 160 (2014) 152–160.
[7] Y. Xiao, X. Sun, l Li, J. Chen, S. Zhao, C. Jiang, L. Yang, L. Cheng, S. Cao, Simultaneous formation of a C/N-TiO2 hollow photocatalyst with efficient photocatalytic performance and recyclability, Chin. J. Catal. 40 (2019) 765–775.
[8] Patent W.O. 2019/ 211787 Nitrogen doped TiO2 nanoparticles and the use thereof in photocatalysis.
[9] M. Chiesa, S. Livraghi, M.C. Paganini, Enrico Salvadori, E. Giamello, Nitrogen-doped semiconducting oxides. Implications on photochemical, photocatalytic and electronic properties derived from EPR spectroscopy, Chem. Sci. 11 (2020) 6623–6641.
[10] C. Di Valentin, G. Pacchioni, A. Selloni, Theory of carbon doping of titanium dioxide, Chem. Mater. 17 (2005) 6656–6665.
[11] C. Di Valentin, E. Finazzi, G. Pacchioni, A. Selloni, S. Livraghi, M.C. Paganini, E. Giamello, N-doped TiO2: theory and experiment, Chem. Phys. 339 (2007) 44–56.
[12] R. Leary, A. Westwood, Carbonaceous nanomaterials for the enhancement of TiO2 photocatalysis, Carbon 49 (2011) 741–772.
[13] J. Yu, S. Wang, J. Low, W. Xiao, Enhanced photocatalytic performance of direct Z-scheme g-C_3N_4-TiO_2 photocatalysts for the decomposition of formaldehyde in air, Phys. Chem. Chem. l Phys. 15 (2013) 16883–16890.
[14] P. Zabek, J. Eberl, H. Kisch, On the origin of visible light activity in carbon-modified titania, Photochem. Photobiol. Sci. 8 (2009) 264–269.
[15] D.M. Tobaldi, M.P. Seabra, G. Otero-Irurueta, Y.R. de Miguel, R.J. Ball, M.K. Singh, R.C. Pullara, J.A. Labrinc, Quantitative XRD characterisation and gas-phase photocatalytic activity testing for visible-light (indoor applications) of KRONOClean 7000®, RSC Adv. 5 (2015), 102911.
[16] R. Quesada-Cabrera, A. Mills, C. O'Rourke, Action spectra of P25 TiO2 and a visible light absorbing, carbon-modified titania in the photocatalytic degradation of stearic acid. Appl. Cat. B Environ. 150– (151) (2014) 338–344.
[17] S. Yin, H. Yamaki, M. Komatsu, Q. Zhang, J. Wang, Q. Tang, F. Saito, T. Sato, Synthesis of visible-light reactive $TiO_{2-x}N_y$ photocatalyst by mechanochemical doping, Solid State Sci. 7 (2005) 1479–1485.
[18] S. Yin, M. Komatsu, Q. Zhang, F. Saito, T. Sato, Synthesis of visible-light responsive nitrogen/carbon doped titania photocatalyst by mechanochemical doping, J. Mater. Sci. 42 (2007) 2399–2404.
[19] R. Rattanakam, S. Supothina, Visible-light-sensitive N-doped TiO_2 photocatalysts prepared by a mechanochemical method: effect of a nitrogen source, Res. Chem. Intermed. 35 (2009) 263–269.
[20] W. Zhong, Y. Yu, C. Du, W. Li, Y. Wang, G. He, Y. Xie, Q. He, Characterization and high pollutant removal ability of buoyant (C, N)–TiO_2/PTFE flakes prepared by high-energy ball-milling, RSC Adv. 4 (2014) 40019–40028.
[21] A.J. Koivisto, K.I. Kling, A.S. Fonseca, A.B. Bluhme, M. Moreman, M. Yud, A. L. Costa, B. Giovanni, S. Ortelli, W. Fransman, U. Vogel, K.A. Jensen, Dip coating of air purifier ceramic honeycombs with photocatalytic TiO2 nanoparticles: a case study for occupational exposure, Sci. Total Environ. 630 (2018) 1283–1291.
[22] E. Arca, G. Mulas, F. Delogu, J. Rodriguez-Ruiz, S. Palma, The influence of mechanical processing on the photoelectrochemical behaviour of TiO_2 powders, J. Alloy. Comp. 477 (2009) 583–587.
[23] Y. Messai, B. Vileno, D. Martel, P. Turek, D.E. Mekki, Milling effect on the photo-activated properties of TiO2 nanoparticles: electronic and structural investigations, Bull. Mater. Sci. 41 (2018) 57.
[24] T. Shinoda, Y. Yamaguchi, A. Kudo, N. Murakami, Photoacoustic spectroscopic analysis of electron-trapping sites in titanium(IV) oxide photocatalyst powder treated by ball milling, J. Phys. Chem. C 126 (2022) 20975–20982.
[25] http://maud.radiographema.eu/.

[26] Patent WO2011/016061PCT Apparatus for determining the residual quantity of polluting agents in a gas mixture and process for determining such quantity.
[27] ISO 22197–1, Fine ceramics (advanced ceramics, advanced technical ceramics) – Test method for air purification performance of semiconducting photocatalytic materials – Part 1: Removal of nitric oxide, first ed., 2007.
[28] S.-C. Zhu, S.-H. Xie, Z.-P. Liu, Nature of rutile nuclei in anatase-to-rutile phase transition, J. Am. Chem. Soc. 137 (2015) 11532–11539.
[29] D.C. Hurum, A.G. Agrios, K.A. Gray, Explaining the enhanced photocatalytic activity of degussa P25 mixed-phase TiO2 using EPR, J. Phys. Chem. B 107 (2003) 4545–4549.
[30] M. Rezaee, S.M.M. Khoie, K.H. Liu, The role of brookite in mechanical activation of anatase-to-rutile transformation of nanocrystalline TiO2: An XRD and Raman spectroscopy investigation, CrystEngComm 13 (2011) 5055.
[31] S.-C. Zhu, S.-H. Xie, Z.-P. Liu, Nature of rutile nuclei in anatase-to-rutile phase transition, J. Am. Chem. Soc. 137 (2015) 11532–11539.
[32] C. Morterra, An infrared spectroscopic study of anatase properties, J. Chem. SOC Faraday Trans. I 84 (1988) 1617–1637.
[33] M. Takeuchi, K. Sakamoto, G. Martra, S. Coluccia, M. Anpo, Mechanism of photoinduced superhydrophilicity on the TiO_2 photocatalyst surface, J. Phys. Chem. B 109 (2005) 15422–15428.
[34] L. Mino, F. Cesano, D. Scarano, G. Spoto, G. Martra, Molecules and heterostructures at TiO_2 surface: the cases of H_2O, CO_2, and organic and inorganic sensitizers, Res. Chem. Intermed. 45 (2019) 5801–5829.
[35] E.A. Konstantinova, A.I. Kokorin, S. Sakthivel, H. Kisch, K. Lips, Carbon doped titanium dioxide, Chimia 61 (2007) 810–814.
[36] S. Livraghi, M.C. Paganini, E. Giamello, A. Selloni, C. Di Valentin, G. Pacchioni, Origin of photoactivity of nitrogen-doped titanium dioxide under visible light, J. Am. Chem. Soc. 128 (2006) 15666–15671.
[37] G. Barolo, S. Livraghi, M. Chiesa, M.C. Paganini, E. Giamello, Mechanism of the photoactivity under visible light of N-doped titanium dioxide. Charge carriers migration in irradiated N-TiO_2 investigated by electron paramagnetic resonance, J. Phys. Chem. C 116 (2012) 20887–20894.
[38] M.M. Ballari, M. Hunger, G. Husken, H.J.H. Brouwers, NOx photocatalytic degradation employing concrete pavement containing titanium dioxide, Appl. Cat. B: Environ. 95 (2010) 245–254.
[39] K. Hadjiivanov, H. Knozinger, Species formed after NO adsorption and NO+ O_2 co-adsorption on TiO_2: an FTIR spectroscopic study, Phys. Chem. Chem. Phys. 2 (2000) 2803–2806.
[40] L. Li, Q. Shen, J. Cheng, Z. Hao, Catalytic oxidation of NO over TiO_2 supported platinum clusters. II: mechanism study by in situ FTIR spectra, Catal. Today 158 (2010) 361–369.
[41] J. Laseka, Y.-H. Yua, J.C.S. Wu, Removal of NOx by photocatalytic processes, J. Photochem. Photobiol. C 14 (2013) 29–52.
[42] J.S. Dalton, P.A. Janes, N.G. Jones, J.A. Nicholson, K.R. Hallam, G.C. Allen, Photocatalytic oxidation of NOx gases using TiO_2: a surface spectroscopic approach, Environ. Pollut. 120 (2002) 415–422.
[43] I.-C. Kang, Q. Zhang, S. Yin, T. Sato, F. Saito, Novel method for preparation of high visible active N-doped TiO_2 photocatalyst with its grinding in solvent, Appl. Cat. B Environ. 84 (2008) 570–576.